Truncation of a Cross-Linked GCN4-p1 Coiled Coil Leads to Ultrafast Folding†

Michelle R. Bunagan,‡ Lidia Cristian,§ William F. DeGrado,‡,§ and Feng Gai*,‡

Department of Chemistry and Department of Biochemistry and Biophysics, University of Pennsylvania, Philadelphia, Pennsylvania 19104

Received March 28, 2006; Revised Manuscript Received July 19, 2006

ABSTRACT: Structural perturbation has been extensively used in protein folding studies because it yields valuable conformational information regarding the folding process. Here we have used N-terminal truncation on a cross-linked variant of the GCN4-p1 leucine zipper, aiming to develop a better understanding of the folding mechanism of the coiled-coil motif. Our results indicate that removing the first heptad repeat in this cross-linked GCN4-p1 coiled coil significantly decreases the folding free energy barrier and results in a maximum folding rate of $(2.0 \pm 0.3\ \mu s)^{-1}$, which is ~50 times faster than that of the full-length protein. Therefore, these results suggest that a set of native or nativelike tertiary interactions, distributed throughout the entire sequence, collectively stabilize the folding transition state of the GCN4-p1 coiled coil. While stable subdomains or triggering sequences have been shown to be critical to the stability of GCN4 coiled coils, our results suggest that the folding of such a subdomain does not seem to dictate the overall folding kinetics.

The GCN4 leucine zipper (e.g., GCN4-p1) derived from yeast transcription activator GCN4 (*1*) is one of the most studied model systems in protein folding. Its folding kinetics and thermodynamics have been studied extensively in the past (*2*−*12*). These studies provided invaluable insights into our understanding of many important factors that govern the folding mechanism and conformational stability of the coiled-coil structural motif. While GCN4-p1 exhibits two-state kinetics in stopped-flow circular dichroism (CD) and fluorescence folding experiments, there is evidence suggesting that one or two folding intermediates may exist at the native side of the major folding barrier (*13*), similar to the so-called hidden intermediate proposed by Bai and co-workers (*14*−*16*). To provide further understanding of the folding mechanism of the coiled-coil motif, we have studied the folding kinetics of a truncated version of GCN4-p1 using the technique of laser-induced temperature jump (*T*-jump)[1] in conjunction with infrared (IR) spectroscopy (*17*).

Structural perturbation by terminal truncation has been used extensively in protein folding studies because it seems to be a valuable tool for identifying conformational clusters that are crucial for folding and stability (*18*, *19*). For example, Nguyen et al. have shown that truncating the C-terminus of a WW domain changes its folding from a three-state mechanism to two-state folding (*20*). On the other hand, in the study of the effect of truncation of the C-terminal helix of the N-terminal domain of ribosomal protein L9 (NTL9), Luisi et al. (*21*) found that the folding rates of $NTL9_{1-51}$ and $NTL9_{1-56}$ are virtually identical while their unfolding rates differ by a factor of 10, indicating that the formation of local structure in the C-terminal helix is not involved in the rate-limiting step for folding. Subsequently, they further showed that even $NTL9_{1-39}$ folds with a rate similar to that of the full-length protein (*22*). In addition, Neira and Fersht (*23*) have used a series of C-terminal fragments of barnase to examine the growth of secondary and tertiary structures. Likewise, truncation has been employed in characterizing the essential dimerization domain responsible for post-translational assembly of selenodeiodinases (*24*) as well as in the study of how conformational space evolves for purified N-terminal polypeptides of increasing length, derived from sperm whale apomyoglobin (*19*).

Similarly, there have been a handful of studies on leucine zipper GCN4-p1 where sequence modification and terminal truncation were employed to dissect the factors that govern the folding and stability of coiled coils. For example, Lumb et al. (*25*) have studied the effect of truncation on the stability of GCN4-p1, at both the N- and C-terminus, and concluded that the leucine zipper coiled coil contains stable subdomains and that the formation of specific tertiary interactions is required for cooperative folding (*26*). Interestingly, their results revealed that $GCN4\text{-}p1_{8-33}$ folds into a coiled-coil structure with substantial stability (the thermal melting temperature at 1 mM is 50 °C), whereas $GCN4\text{-}p1_{11-33}$ is predominantly unfolded, even at 0 °C. Since full-length GCN4-p1 seems to fold via a rather complicated mechanism (*13*), it would therefore be interesting to study the folding kinetics of those truncated GCN4-p1 peptides identified by Lumb et al. (*25*) and to examine if their folding mechanisms differ from that of the full-length protein. Such studies would help us to understand, from a kinetic point of view, why those short coiled-coil peptides dimerize and what factors control their folding rate. Among those that were studied, $GCN4\text{-}p1_{8-33}$ appears to be the most interesting because

† Supported by NIH Grant GM-065978.

* To whom correspondence should be addressed. Telephone: (215) 573-6256. Fax: (215) 573-2112. E-mail: gai@sas.upenn.edu.

‡ Department of Chemistry.

§ Department of Biochemistry and Biophysics.

[1] Abbreviations: *T*-Jump, temperature jump; MALDI-TOF, matrix assisted laser desorption and ionization - time of flight; CD, circular dichroism; NMR, nuclear magnetic resonance; FTIR, Fourier transform infrared

10.1021/bi0606142 CCC: $33.50
Published on Web 08/23/2006

Zitzewitz et al. (*10*) have shown that the two C-terminal heptads are the likely source of the nucleating helices in GCN4-p1.

Specifically, we have studied a truncated, cross-linked variant of the GCN4-p1 leucine zipper, i.e., GCN4-p1$_{9-35}$-c″, which is similar to those used by Wang et al. (*13*) as well as Sosnick and co-workers (*6*, *27*). This covalently linked homodimer, which has a disulfide cross-linker at the C-terminus, was prepared by linking two truncated monomers (i.e., GCN4-p1$_{9-35}$) together via a disulfide bond formed between two cysteine residues (*6*, *28*). An advantage of cross-linking two helices together is that it eliminates the bimolecular collision process encountered by the dimeric forms of GCN4-p1, thereby simplifying the interpretation of the experimental results. In addition, Sosnick and co-workers (*6*, *27*) have recently shown that an unstructured cross-linker can lead to a more structurally homogeneous folding transition state for the folding of coiled coils, compared to that of unlinked monomers.

The *T*-jump-induced relaxation kinetics of this monomeric coiled coil, obtained by monitoring the amide I′ infrared band of the polypeptide backbone, can be described by a single-exponential function. Compared to that of the full-length GCN4-p1 coiled coil (*13*), its folding time is drastically shortened. For example, at 70 °C, the folding time of GCN4-p1$_{9-35}$-c″ is ~2.1 μs, which makes it one of the fastest known protein folders (*29*−*32*).

MATERIALS AND METHODS

Peptide Synthesis and Purification. The GCN4 peptide used in this study has the following sequence with the cross-linker underlined: VEELLSKNWH^{10} LENEVARLKK^{20} LVKQGGC. This peptide corresponds to an N-terminally truncated variant of the GCN4-p1-c″ monomer (*6*, *27*) with its first heptad repeat removed and was synthesized using the standard solid-phase 9-fluorenylmethoxycarbonyl (Fmoc) method. Before purification, the Cys was reduced to the thiol by reaction with tris(2-carboxyethyl)phosphine hydrochloride (TCEP·HCl), and the resultant sample was purified by reverse-phase HPLC with a C18 column. The corresponding homodimer (i.e., GCN4-p1$_{9-35}$-c″) was prepared by cross-linking the individual polypeptide chains by stirring the peptide solution with 10 mM ammonium bicarbonate at pH 8.0 overnight. The disulfide-bonded peptide was then purified by reverse-phase HPLC and its identity confirmed by MALDI-TOF mass spectrometry.

Sample Preparation. As described in detail elsewhere (*17*), multiple rounds of lyophilization were performed to remove the trifluoroacetic acid (TFA) from peptide purification and also the exchangeable protons of the peptide. For circular dichroism (CD) and IR experiments, the solution was prepared by directly dissolving the lyophilized samples in 20 mM (CD) and 50 mM (IR) sodium phosphate/D_2O buffers (pH* 7.0), respectively. The concentration of the sample was determined by the absorbance at 282 nm, using an extinction coefficient of 11 200 cm^{-1} M^{-1}. The final concentration was ~30 μM for CD and ~1.0 mM for IR.

CD Spectroscopy. Both wavelength scan and thermal melting CD curves were collected on an Aviv 62A DS circular dichroism spectrometer (Aviv Associates, Lakewood, NJ) using a 1 mm sample cuvette. The folding−unfolding thermodynamics of GCN4-p1$_{9-35}$-c″ were obtained by fitting its CD thermal melting transition obtained at 222 nm to the following two-state model:

$$\theta(T) = \frac{\theta_F(T) + K_{eq}(T) \times \theta_U(T)}{1 + K_{eq}(T)} \quad (1)$$

$$K_{eq}(T) = \exp[-\Delta G(T)/RT] \quad (2)$$

$$\Delta G(T) = \Delta H_m + \Delta C_p(T - T_m) - T[\Delta S_m + \Delta C_p \ln(T/T_m)] \quad (3)$$

where $\theta_F(T)$ is the folded CD baseline, $\theta_U(T)$ is the unfolded CD baseline, $K_{eq}(T)$ is the equilibrium constant for unfolding, T_m equals $\Delta H_m/\Delta S_m$ and is the thermal melting temperature, ΔH_m and ΔS_m are the enthalpy and entropy changes at T_m, respectively, and ΔC_p is the heat capacity change associated with unfolding, which has been assumed here to be temperature-independent. In the fit, $\theta_F(T)$ was treated as a linear function of temperature, whereas $\theta_U(T)$, which was also assumed to be a linear function of temperature, was determined from the CD signal of GCN4-p1$_{9-35}$-c″ in 3.0 M guanidinium hydrochloride (GuHCl).

NMR Spectroscopy. The one-dimensional NMR spectra of GCN4-p1$_{9-35}$-c″ were collected on a Bruker DMX 600 MHz spectrometer at 25 °C. The concentration of the sample was ~1 mg/mL in a H_2O/D_2O phosphate buffer solution (20 mM, pH 7).

Fluorescence Spectroscopy. Fluorescence spectra were recorded on a Fluorolog 3.10 spectrofluorometer (Jobin Yvon Horiba) with 1 nm spectral resolution (excitation and emission) and a 1 cm quartz sample cuvette. The temperature was regulated using a TLC 50 Peltier temperature controller (Quantum Northwest). The sample was prepared by directly dissolving lyophilized peptide into 40 mM phosphate buffer (pH 7), and the final concentration was ~9 μM.

Fourier Transform Infrared (FTIR) Spectroscopy. Static FTIR spectra were collected on a Magna-IR 860 spectrometer equipped with a HgCdTe detector using 2 cm^{-1} resolution. A homemade CaF_2 sample cell that was divided into two compartments with a 52 μm Teflon spacer and mounted on a programmable translation stage was used to allow separate measurements of the sample and the reference under identical conditions. Temperature control with a precision of ±0.2 °C was obtained with a thermostated copper block. Typically, 256 scans were averaged to generate one spectrum.

Time-Resolved T-Jump IR Spectroscopy. The *T*-jump technique uses a burst of energy to heat up a sample solution within a very short period of time, i.e., a few nanoseconds. As a result, the sudden increase in temperature induces a population redistribution among conformational ensembles that are initially at equilibrium. Hence, the time course in which the nonequilibrium state evolves toward a new equilibrium position contains information regarding the kinetics of folding and unfolding. The time-resolved *T*-jump IR apparatus used in this study has been described in detail elsewhere (*17*). Briefly, a 1.9 μm laser pulse, generated via Raman shifting of the fundamental output of a Q-switched Nd:YAG laser in H_2, was used to generate a 8−10 °C *T*-jump, and the *T*-jump-induced transient absorbance changes were measured by a continuous wave (CW) IR diode laser

in conjunction with a 50 MHz HgCdTe detector and a digital oscilloscope. A thermostated, two-compartment sample cell with a path length of 52 μm was used to allow the separate measurements of the sample and buffer under identical conditions. The measurements with buffer provide information for both background subtraction and *T*-jump amplitude determination. The latter was achieved by using the *T*-jump-induced absorbance change of the D_2O buffer solution at probing frequency ν, $\Delta A(\Delta T,\nu)$, and the equation $\Delta A(\Delta T,\nu) = a(\nu)\Delta T + b(\nu)\Delta T^2$, where ΔT corresponds to the difference between the final (T_f) and initial (T_i) temperatures and $a(\nu)$ and $b(\nu)$ are constants that were determined by analyzing the temperature dependence of the FTIR spectra of the buffer.

RESULTS

CD Spectroscopy. Consistent with the result of Cristian et al. (*33*), the CD spectrum of the GCN4-p1$_{9-35}$-c″ monomer (without the disulfide cross-linker) showed that it is predominantly unfolded at 25 °C (data not shown). However, cross-linking two GCN4-p1$_{9-35}$ monomers together in a parallel fashion via a disulfide bond results in a more stable coiled coil (*33*, *34*). As shown (Figure 1a), the far-UV CD spectrum of GCN4-p1$_{9-35}$-c″ exhibits the characteristics of α-helical proteins, with double minima at 208 and 222 nm. However, its mean residue ellipticity at a low temperature (e.g., 4 °C) is smaller than that of GCN4-p1-c″ (*13*, *33*), suggesting that the N-terminus of the helices is probably frayed, most likely due to the unblocked N-terminus. Lumb et al. (*25*) have shown that acetylation of the N-terminus of GCN4-p3 results in a more stable coiled-coil structure and consequently higher helicity. Nevertheless, temperature-dependent CD measurements indicated that GCN4-p1$_{9-35}$-c″ undergoes a cooperative thermal unfolding transition with an increase in temperature (Figure 1b). Further analysis employing a two-state model indicated that the thermal melting temperature of GCN4-p1$_{9-35}$-c″ is ∼70 °C, which is ∼18 °C lower than that of the corresponding full-length peptide (*13*). Presumably, this decrease in stability is caused by the terminal truncation.

NMR Spectroscopy. The amide NH and aromatic region of the one-dimensional ^{1}H NMR spectrum of GCN4-p1$_{9-35}$-c″ collected at 25 °C shows well-dispersed lines (Figure 2), suggesting that the peptide is folded at this temperature. In addition, this spectrum is similar to that of GCN4-p1$_{8-33}$, which has been shown by Lumb et al. (*25*) to adopt a coiled-coil conformation in aqueous solution.

Fluorescence Spectroscopy. Trp fluorescence has been extensively used in the study of the folding properties of GCN4-p1 coiled coils (*4*, *6*, *27*). Herein, we have also attempted to use Trp fluorescence as an additional means of understanding the folding mechanism of GCN4-p1$_{9-35}$-c″. However, we found that the fluorescence spectrum of GCN4-p1$_{9-35}$-c″ peaks at ∼356 nm at 20 °C (data not shown), suggesting that the Trp side chains are largely exposed and solvated. Therefore, they are not good probes for folding studies. Further titration studies using both temperature and urea as "denaturants" also corroborate this idea.

T-Jump IR Study. The *T*-jump-induced relaxation kinetics of the GCN4-p1$_{9-35}$-c″ coiled coil were monitored by time-resolved IR spectroscopy using a probing frequency of 1633 cm^{-1} (*17*). This value was chosen because it has been shown

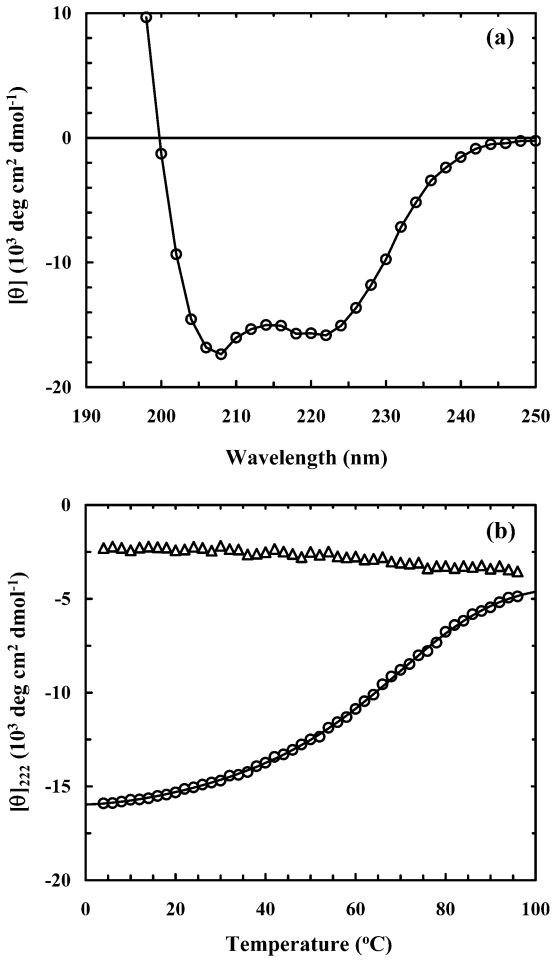

FIGURE 1: (a) Far-UV CD spectrum of GCN4-p1$_{9-35}$-c″ at 25 °C. (b) Temperature-dependent mean residue ellipticities of GCN4-p1$_{9-35}$-c″ in aqueous solution at 222 nm (○). Fitting these data to an apparent two-state model (—), i.e., eqs 1−3, yielded the following thermodynamic parameters for unfolding: $\Delta H_m = 16.5 \pm 1.0$ kcal/mol, $\Delta S_m = 48.0 \pm 2.3$ cal K^{-1} mol^{-1}, $\Delta C_p = 284 \pm 18$ cal K^{-1} mol^{-1}, and $T_m = 70.1 \pm 0.3$ °C. Also shown are the temperature-dependent mean residue ellipticities of GCN4-p1$_{9-35}$-c″ in a 3.0 M GuHCl solution at 222 nm (△), which were used to determine the unfolded CD baseline.

that the fully and/or partially solvated helical amides absorb near this frequency (*31*, *32*, *35*). Indeed, the difference FTIR spectra of GCN4-p1$_{9-35}$-c″ (Figure 3) show that a negative-going band, centered at ∼1630 cm^{-1}, increases with an increase in temperature. While this result is consistent with the CD thermal melting data, no attempt was made to extract folding thermodynamics from these FTIR spectra. Nevertheless, it is worth pointing out that these FTIR data suggest that no detectable (by the current method) aggregation occurs even at the highest temperature (i.e., ∼91 °C), as judged by the lack of distinct spectral features (*36*) associated with aggregates at 1618 and 1680 cm^{-1}.

As shown (Figure 4), the *T*-jump-induced relaxation kinetics exhibit two phases. The fast phase, which is unresolved in time due to the 10−15 ns response time of the IR detection system, is likely due to temperature-induced spectral changes discussed previously (*17*). Other factors, such as helix fraying (*12*) and imperfect background subtraction, could also contribute to this phase. On the other hand, the slow phase is on the microsecond time scale and thereby well-resolved. Although we cannot completely rule out the

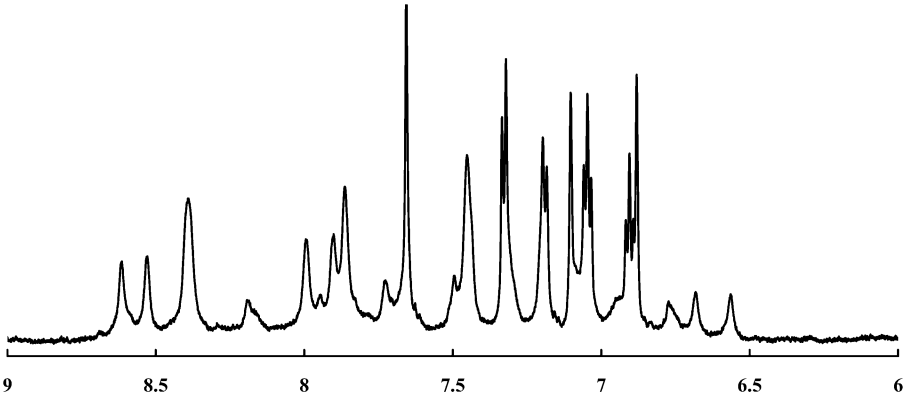

FIGURE 2: One-dimensional ^{1}H NMR spectrum of GCN4-p1$_{9-35}$-c″ recorded at 25 °C.

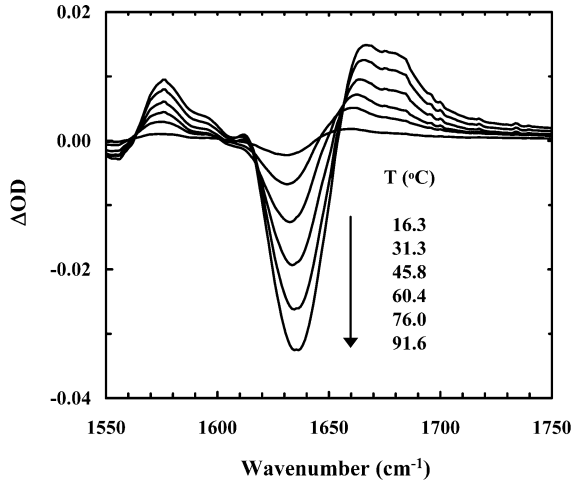

FIGURE 3: Difference FTIR spectra of GCN4-p1$_{9-35}$-c″ (in the amide I′ region). These spectra were generated by subtracting the FTIR spectrum of GCN4-p1$_{9-35}$-c″ collected at 8.8 °C from those collected at higher temperatures, as indicated.

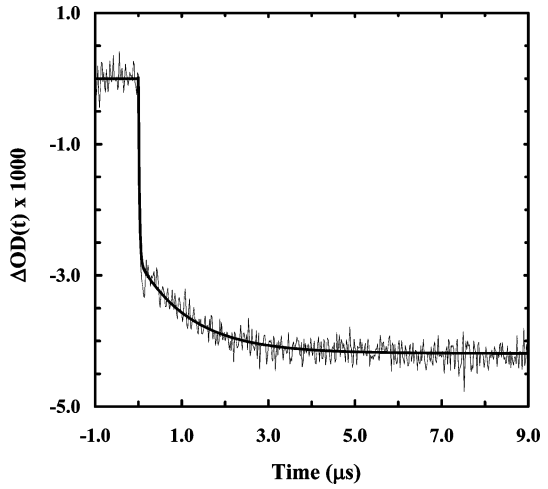

FIGURE 4: Representative *T*-jump-induced relaxation trace of GCN4-p1$_{9-35}$-c″ in response to a *T*-jump of 8.4 °C, from 58.7 to 67.1 °C. The smooth line is a fit of these data to the function $\Delta OD(t) = A[1 - B \exp(-t/\tau)]$, where $A = -4.2$, $B = 0.33$, and $\tau = 1.2$ μs.

possibility that even longer relaxation events exist, the fact that the kinetic amplitude at the longest decay time matches quite well with the equilibrium amplitude (data not shown) suggests that there is no significant change in the IR absorbance at the probing frequency occurring on the millisecond or longer time scale. The slow relaxation phase

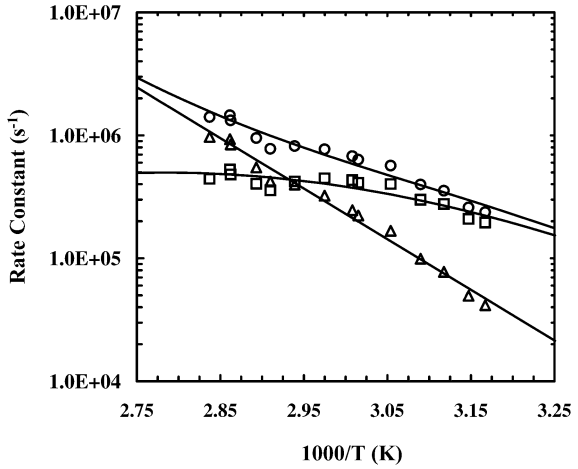

FIGURE 5: Arrhenius plot of the observed relaxation rate constant (□) as well as the folding (○) and unfolding (△) rate constants of GCN4-p1$_{9-35}$-c″. Lines are fits to the Eyring equation.

can be modeled by a single-exponential function and therefore suggests that folding proceeds along a pathway involving only one dominant free energy barrier. In this case, the observed relaxation rate constant (k_r) is equal to the sum of the folding (k_f) and unfolding (k_u) rate constants (i.e., $k_r = k_f + k_u$). Knowledge of the equilibrium constant corresponding to the final temperature allows determination of k_f and k_u, since $K_{eq} = k_f/k_u$. Thus, using the unfolding thermodynamic parameters obtained from CD and the observed relaxation rate constants, we were able to determine the temperature dependence of the folding and unfolding rates of GCN4-p1$_{9-35}$-c″ (Figure 5). Similar to that often observed for protein folding, the folding rate constant of GCN4-p1$_{9-35}$-c″ exhibits a concave-down dependence on temperature. In addition, the folding of GCN4-p1$_{9-35}$-c″ is very fast; for instance, its folding rate at 70 °C is $(2.1 \pm 0.3$ $\mu s)^{-1}$, one of the fastest known folding rates (*29*−*32*). Finally, it is worth noting that monomeric helices fold on a much faster time scale near this temperature (*17*, *37*, *38*), and therefore, the folding rate discussed above should be characteristic of the folding kinetics of the coiled-coil structure.

DISCUSSION

The folding kinetics of GCN4 coiled coils have been studied extensively using stopped-flow fluorescence (*2*−*4*, *6*, *27*) and CD (*10*, *11*, *39*) techniques. The majority of these studies reported two-state folding kinetics and thereby

supported the idea that the folding of coiled coils is a two-state-like process, wherein only one dominant free energy barrier separates the unfolded monomers from the folded dimer. Additionally, a number of equilibrium unfolding studies (*11*, *40*) also suggested that an apparent two-state model could adequately describe the thermal as well as chaotropic folding−unfolding transitions of GCN4 coiled coils. On the other hand, Wang et al. (*13*) have recently shown that the folding mechanism of two cross-linked variants of the GCN4-p1 coiled coil may be more complicated than a folding pathway in which only two conformational ensembles are involved, as indicated by the non-monoexponential relaxation kinetics of these molecules in response to a *T*-jump. Their study is consistent with a scenario in which an intermediate exists at the native side of the rate-limiting step (*14*−*16*). The idea that the folding of the GCN4 coiled coil is a multistate process has also been suggested in a previous study by Dragan and Privalov (*12*), who identified three transitions in the thermal unfolding of GCN4-p1.

Consistent with other studies (*25*, *41*), our results indicate that N-terminal truncation of GCN4-p1 peptides results in a less stable coiled coil. Compared to that of full-length GCN4-p1-c″, the thermal melting temperature of GCN4-p1$_{9-35}$-c″ is decreased by ∼18 °C (*13*). Therefore, these results support the notion that the heptad repeats in GCN4 coiled coils collectively stabilize the tertiary fold (*1*). Furthermore, our results showed that the disulfide cross-linker, which leads to a relatively high effective concentration of the monomers (*6*), plays a stabilizing role. Interestingly, however, N-terminal truncation of the same GCN4-p1-c″ used by Wang et al. leads to not only simpler folding kinetics but also an ultrafast folding rate. For example, the folding time of GCN4-p1$_{9-35}$-c″ at 70 °C is 2.1 ± 0.3 μs, whereas the overall folding time of GCN4-p1-c″ at the same temperature is ∼100 μs (*13*). Thus, these results also have important ramifications for understanding the folding mechanism of the GCN4-p1 coiled coil.

First, these results indicate that the size or chain length is an important determinant of the folding free energy landscape and, therefore, the folding pathway as well as the overall folding rate of GCN4 coiled coils. While chain length-dependent folding kinetics have also been observed in other studies (*37*, *42*−*45*) and our results are consistent with those of Thirumalai and co-workers (*42*, *44*), the finding presented here should not be generalized to other proteins. As a matter of fact, Raleigh and co-workers (*21*, *22*) have shown that truncating the N-terminal domain of ribosomal protein L9 does not alter its folding kinetics. Nevertheless, given the fact that GCN4-p1-c″ and GCN4-p1$_{9-35}$-c″ have similar contact orders, it is not surprising that chain length can play a dominant role in determining the comparative folding rates of these coiled coils. Furthermore, the ultrafast folding behavior of GCN4-p1$_{9-35}$-c″ is in agreement with the study of Zitzewitz et al. (*10*), who have shown that the 10-residue sequence at the C-terminus of GCN4-p1 plays a critical role in triggering helix initiation and tertiary structure formation.

Second, these results suggest that the folding transition state ensemble of full-length GCN4-p1-c″ contains critical native or nativelike tertiary interactions throughout the entire chain, consistent with the notion that tertiary interactions play an important role in the folding of the coiled-coil structures (*25*). Otherwise, GCN4-p1$_{9-35}$-c″ and GCN4-p1-c″ would fold with similar rates. In other words, the folding transition states of truncated and full-length GCN4-p1-c″ are different, suggesting that the formation of a nativelike segment or subdomain in GCN4-p1 is probably necessary but not sufficient to stabilize the folding transition state. Therefore, these results are consistent with the folding mechanism proposed by Wang et al. (*13*), who suggested that the major folding transition barrier in the folding of full-length GCN4-p1-c″ arises from the cooperative association of the two strands, and also the results of Durr et al. (*46*), who showed that strengthening the hydrophobic interactions throughout the sequence of a modified GCN4-p1 coiled coil increases the folding rate by ∼20-fold, although the calculated helical propensity of the monomer is ∼10 times lower than that of GCN4-p1 (*6*).

Furthermore, these results, although in an indirect manner, are in accord with the interpretation of Wang et al., who attributed the complex relaxation kinetics of GCN4-p1-c″ to folding and unfolding, but not to aggregation. Since GCN4-p1$_{9-35}$-c″ is less stable than its full-length counterpart, it would have been easier to observe aggregate formation for the truncated variant in the temperature range in which the *T*-jump data were collected. However, no long relaxation components (e.g., tens and hundreds of microseconds) were observed in the relaxation kinetics of GCN4-p1$_{9-35}$-c″. Finally, the shorter sequence and ultrafast folding rate make GCN4-p1$_{9-35}$-c″ an ideal model system for computer simulation studies.

In light of these findings, it would be interesting to study the folding mechanism of a C-terminally truncated GCN4-p1 coiled coil. However, results of previous studies suggest that such a peptide is unlikely to fold (*10*, *25*, *41*). Therefore, no attempt was made to investigate the folding kinetics of such a system. Additionally, more sophisticated NMR techniques should be used in the future to investigate the structure and side chain dynamics of GCN4-p1$_{9-35}$-c″. If the side chain packing in the truncated protein is significantly different from that of the full-length protein, an alternative interpretation of the ultrafast folding behavior of GCN4-p1$_{9-35}$-c″ would be needed.

CONCLUSIONS

In summary, we have studied the thermal stability and folding kinetics of a truncated, cross-linked variant of the GCN4-p1 leucine zipper using static CD, NMR, and infrared spectroscopies as well as a time-resolved *T*-jump infrared technique. Our results indicate that removal of the first heptad repeat decreases the stability of the coiled-coil structure. However, such a truncation also significantly decreases the folding free energy barrier, leading to ultrafast folding. Taken together, these results suggest a folding mechanism in which a set of tertiary interactions, distributed throughout the entire sequence, collectively stabilize the folding transition state of the GCN4-p1 coiled coil. While stable subdomains or triggering sequences have been shown to be critical structure elements in GCN4 coiled coils, the formation of such a subdomain does not appear to be sufficient to drive the system across the folding free energy barrier.

REFERENCES

1. O'Shea, E. K., Klemm, J. D., Kim, P. S., and Alber, T. (1991) X-ray structure of the GCN4 leucine zipper, a two-stranded, parallel coiled coil, *Science 254*, 539−544.

2. Wendt, H., Baici, A., and Bosshard, H. R. (1994) Mechanism of assembly of a leucine zipper domain, *J. Am. Chem. Soc. 116*, 6973−6974.
3. Wendt, H., Berger, C., Baici, A., Thomas, R. M., and Bosshard, H. R. (1995) Kinetics of folding of leucine zipper domains, *Biochemistry 34*, 4097−4107.
4. Sosnick, T. R., Jackson, S., Wilk, R. R., Englander, S. W., and DeGrado, W. F. (1996) The role of helix formation in the folding of a fully α-helical coiled coil, *Proteins 24*, 427−432.
5. Holtzer, M. E., Lovett, E. G., d'Avignon, D. A., and Holtzer, A. (1997) Thermal unfolding in a GCN4-like leucine zipper: $^{13}C^{\alpha}$ NMR chemical shifts and local unfolding curves, *Biophys. J. 73*, 1031−1041.
6. Moran, L. B., Schneider, J. P., Kentsis, A., Reddy, G. A., and Sosnick, T. R. (1999) Transition state heterogeneity in GCN4 coiled coil folding studied by using multisite mutations and crosslinking, *Proc. Natl. Acad. Sci. U.S.A. 96*, 10699−10704.
7. Jia, Y., Talaga, D. S., Lau, W. L., Lu, H. S. M., DeGrado, W. F., and Hochstrasser, R. M. (1999) Folding dynamics of single GCN4 peptides by fluorescence resonant energy transfer confocal microscopy, *Chem. Phys. 247*, 69−83.
8. Myers, J. K., and Oas, T. G. (1999) Reinterpretation of GCN4-p1 folding kinetics: Partial helix formation precedes dimerization in coiled coil folding, *J. Mol. Biol. 289*, 205−209.
9. Mohanty, D., Kolinski, A., and Skolnick, J. (1999) De novo simulations of the folding thermodynamics of the GCN4 leucine zipper, *Biophys. J. 77*, 54−69.
10. Zitzewitz, J. A., Ibarra-Molero, B., Fishel, D. R., Terry, K. L., and Matthews, C. R. (2000) Preformed secondary structure drives the association reaction of GCN4-p1, a model coiled-coil system, *J. Mol. Biol. 296*, 1105−1116.
11. Ibarra-Molero, B., Makhatadze, G. I., and Matthews, C. R. (2001) Mapping the energy surface for the folding reaction of the coiled-coil peptide GCN4-p1, *Biochemistry 40*, 719−731.
12. Dragan, A. I., and Privalov, P. L. (2002) Unfolding of a leucine zipper is not a simple two-state transition, *J. Mol. Biol. 321*, 891−908.
13. Wang, T., Lau, W. L., DeGrado, W. F., and Gai, F. (2005) *T*-Jump infrared study of the folding mechanism of coiled-coil GCN4-p1, *Biophys. J. 89*, 4180−4187.
14. Bai, Y. (2003) Hidden intermediates and Levinthal paradox in the folding of small proteins, *Biochem. Biophys. Res. Commun. 305*, 785−788.
15. Bai, Y., Sosnick, T. R., Mayne, L., and Englander, S. W. (1995) Protein folding intermediates: Native-state hydrogen exchange, *Science 269*, 192−197.
16. Takei, J., Pei, W., Vu, D., and Bai, Y. (2002) Populating partially unfolded forms by hydrogen exchange-directed protein engineering, *Biochemistry 41*, 12308−12312.
17. Huang, C.-Y., Getahun, Z., Zhu, Y., Klemke, J. W., DeGrado, W. F., and Gai, F. (2002) Helix formation via conformation diffusion search, *Proc. Natl. Acad. Sci. U.S.A. 99*, 2788−2793.
18. Neira, J. L., and Fersht, A. R. (1999) Exploring the folding funnel of a polypeptide chain by biophysical studies on protein fragments, *J. Mol. Biol. 285*, 1309−1333.
19. Chow, C. C., Chow, C., Raghunathan, V., Huppert, T. J., Kimball, E. B., and Cavagnero, S. (2003) Chain length dependence of apomyoglobin folding: Structural evolution from misfolded sheets to native helices, *Biochemistry 42*, 7090−7099.
20. Nguyen, H., Jäger, M., Moretto, A., Gruebele, M., and Kelly, J. W. (2003) Tuning the free-energy landscape of a WW domain by temperature, mutation, and truncation, *Proc. Natl. Acad. Sci. U.S.A. 100*, 3948−3953.
21. Luisi, D. L., Kuhlman, B., Sideras, K., Evans, P. A., and Raleigh, D. P. (2002) Effects of varying the local propensity to form secondary structure on the stability and folding kinetics of a rapid folding mixed α/*β* protein: Characterization of a truncation mutant of the N-terminal domain of the ribosomal protein L9, *J. Mol. Biol. 289*, 167−174.
22. Horng, J.-C., Moroz, V., and Raleigh, D. P. (2003) Rapid cooperative two-state folding of a miniature α−*β* protein and design of a thermostable variant, *J. Mol. Biol. 326*, 1261−1270.
23. Neira, J. L., and Fersht, A. R. (1999) Acquisition of native-like interactions in C-terminal fragments of barnase, *J. Mol. Biol. 287*, 421−432.
24. Leonard, J. L., Simpson, G., and Leonard, D. M. (2005) Characterization of the protein dimerization domain responsible for assembly of functional selenodeiodinases, *J. Biol. Chem. 280*, 11093−11100.
25. Lumb, K. J., Carr, C. M., and Kim, P. S. (1994) Subdomain folding of the coiled coil leucine zipper from the bZIP transcriptional activator GCN4, *Biochemistry 33*, 7361−7367.
26. Goodman, E. M., and Kim, P. S. (1991) Periodicity of amide proton exchange rates in a coiled-coil leucine zipper peptide, *Biochemistry 30*, 11615−11620.
27. Krantz, B. A., and Sosnick, T. R. (2001) Engineered metal binding sites map the heterogeneous folding landscape of a coiled coil, *Nat. Struct. Biol. 8*, 1042−1047.
28. O'Shea, E. K., Rutkowski, R., and Kim, P. S. (1989) Evidence that the leucine zipper is a coiled coil, *Science 243*, 538−542.
29. Kubelka, J., Hofrichter, J., and Eaton, W. A. (2004) The protein folding 'speed limit', *Curr. Opin. Struct. Biol. 14*, 76−88.
30. Mayor, U., Johnson, C. M., Daggett, V., and Fersht, A. R. (2000) Protein folding and unfolding in microseconds to nanoseconds by experiment and simulation, *Proc. Natl. Acad. Sci. U.S.A. 97*, 13518−13522.
31. Zhu, Y., Alonso, D. O. V., Maki, K., Huang, C.-Y., Lahr, S. J., Daggett, V., Roder, H., DeGrado, W. F., and Gai, F. (2003) Ultrafast folding of α_3D: A *de novo* designed three-helix bundle protein, *Proc. Natl. Acad. Sci. U.S.A. 100*, 15486−15491.
32. Zhu, Y., Fu, X., Wang, T., Tamura, A., Takada, S., Saven, J. G., and Gai, F. (2004) Guiding the search for a protein's maximum rate of folding, *Chem. Phys. 307*, 99−109.
33. Cristian, L., Nanda, V., Lear, J. D., and DeGrado, W. F. (2005) Synergistic interactions between aqueous and membrane domains of a designed protein determine its fold and stability, *J. Mol. Biol. 348*, 1225−1233.
34. Zhou, N. E., Kay, C. M., and Hodges, R. S. (1993) Disulfide bond contribution to protein stability: Positional effects of substitution in the hydrophobic core of the 2-stranded α-helical coiled-coil, *Biochemistry 32*, 3178−3187.
35. Walsh, S. T. R., Cheng, R. P., Wright, W. W., Alonso, D. O. V., Daggett, V., Vanderkooi, J. M., and DeGrado, W. F. (2003) The hydration of amides in helices: A comprehensive picture from molecular dynamics, IR, and NMR, *Protein Sci. 12*, 520−531.
36. Timasheff, S. N., Susi, H., and Stevens, L. J. (1967) Infrared spectra and protein conformations in aqueous solutions. 2. Survey of globular proteins, *Biol. Chem. 242*, 5467−5473.
37. Wang, T., Zhu, Y., Getahun, Z., Du, D., Huang, C.-Y., DeGrado, W. F., and Gai, F. (2004) Length dependent helix-coil transition kinetics of nine alanine-based peptides, *J. Phys. Chem. B 108*, 15301−15310.
38. Wang, T., Du, D. G., and Gai, F. (2003) Helix-coil kinetics of two 14-residue peptides, *Chem. Phys. Lett. 370*, 842−848.
39. Zitzewitz, J. A., Bilsel, O., Luo, J. B., Jones, B. E., and Matthews, C. R. (1995) Probing the folding mechanism of a leucine-zipper peptide by stopped-flow circular-dichroism spectroscopy, *Biochemistry 34*, 12812−12819.
40. Thompson, K. S., Vinson, C. R., and Freire, E. (1993) Thermodynamic characterization of the structural stability of the coiled-coil region of the bZIP transcription factor GCN4, *Biochemistry 32*, 5491−5496.
41. Kammerer, R. A., Schulthess, T., Landwehr, R., Lustig, A., Engel, J., Aebi, U., and Steinmetz, M. O. (1998) An autonomous folding unit mediates the assembly of two-stranded coiled coils, *Proc. Natl. Acad. Sci. U.S.A. 95*, 13419−13424.
42. Thirumalai, D., and Klimov, D. K. (1999) Deciphering the timescales and mechanisms of protein folding using minimal off-lattice models, *Curr. Opin. Struct. Biol. 9*, 197−207.
43. Koga, N., and Takada, S. (2001) Roles of native topology and chain-length scaling in protein folding: A simulation study with a Go-like model, *J. Mol. Biol. 313*, 171−180.
44. Li, M. S., Klimov, D. K., and Thirumalai, D. (2004) Thermal denaturation and folding rates of single domain proteins: Size matters, *Polymer 45*, 573−579.
45. Kouza, M., Li, M. S., O'Brien, E. P., Jr., Hu, C.-H., and Thirumalai, D. (2006) Effect of finite size on cooperativity and rates of protein folding, *J. Phys. Chem. A 110*, 671−676.
46. Durr, E., Jelesarov, I., and Bosshard, H. R. (1999) Extremely fast folding of a very stable leucine zipper with a strengthened hydrophobic core and lacking electrostatic interactions between helices, *Biochemistry 38*, 870−880.

BI0606142